THE ASTROPHYSICAL JOURNAL, 441:L77–L80, 1995 March 10

THE HOMUNCULUS OF η CARINAE: AN INTERACTING STELLAR WINDS PARADIGM

ADAM FRANK,[1] BRUCE BALICK,[2] AND KRIS DAVIDSON[1]

Received 1994 September 9; accepted 1994 December 19

ABSTRACT

We simulate the origin and evolution of the bipolar nebula surrounding η Car using numerical two-dimensional gasdynamical models. The generalized interacting stellar winds scenario, wherein a stellar wind interacts with an aspherical circumstellar environment, is adopted. The eruption wind of 1840–1860, which is taken to be spherically symmetric, interacts with a preeruption toroidal density environment. Using reasonable assumptions of initial conditions and eruption parameters based on archival data, we have performed over 30 simulations in an effort to bracket the initial parameters which produce models that best match observations. We find that models with high pole-to-equator density contrasts (>100) and toroidal density configurations nicely account for the observed morphology and kinematics of the homunculus.

Subject headings: hydrodynamics — shock waves — stars: individual (η Carinae) — stars: mass loss

1. INTRODUCTION

Recent *HST* images of the inner nebula, or homunculus, surrounding the star η Carinae (Ebbets et al. 1994a, b; cf. Hester et al. 1991; Davidson 1993) reveal its striking bipolar morphology. The homunculus displays two nearly circular lobes joined at a narrow waist which appears to be surrounded by a gaseous disk (see Fig. 1). A complex distribution of dust and gas, including amorphous and jetlike components, surrounds the homunculus (Meaburn, Walsh, & Wolstencroft 1993).

The star η Car, the central star whose winds are the driving source of the bipolar nebula, is itself an intriguing object. A massive star (Humphreys & Davidson 1994) classified as a luminous blue variable (LBV), η Car became the second brightest star in the sky during a 20 year eruption in the mid-nineteenth century ($\sim$1840–1860). It is still one of the most luminous stars observed and is known to be producing a fast, massive stellar wind (Damineli Neto et al. 1993). Although it is not considered typical of the class, η Car has been an ideal laboratory for understanding the properties of LBVs because of its relative proximity, high luminosity, and volatile nature.

By revealing both the macro and microstructure of the bipolar homunculus, the new *HST* images now make η Car an ideal laboratory for understanding the history of LBVs, their winds, and the interactions of these winds with the local environment. If the morphology and kinematics of the bipolar nebula could be linked to a unique family of formation mechanisms, then the nebular properties might be used as diagnostics of evolutionary scenarios for both the star and its wind/eruptions. In this *Letter* we present the first results of a campaign to understand the bipolar nebula surrounding η Car through a program of gasdynamic numerical simulations.

2. CRITICAL OBSERVATIONS

LBVs are known to lose mass in the form of steady stellar winds punctuated by eruptive events where the mass loss increases dramatically for a short period of time (Maeder 1989). Based on the mass in the nebula, it is believed that during the 20 year eruption in the mid-nineteenth century the mass-loss rate from η Car was as high as a few solar masses per decade! The velocity of the wind during the eruption is not known but can be inferred from current kinematics to $\sim$800 km s^{-1} (Lamers 1989).

Today, in its period of relative quiescence, it is clear that η Car is currently losing mass in the form of a relatively dense high-velocity wind (5×10^{-4} $M_\odot$ yr^{-1}, $v \sim 700$ km s^{-1}; Lamers 1989). Based on observations of other LBVs, it is reasonable to assume that a wind with similar properties existed before the last eruption (Humphreys & Davidson 1994).

While the macroscopic features—the bipolar lobes and disk—appear remarkably well defined, the entire nebula shows an extraordinary amount of fine-scale detail such as knots, blobs, and cometary tails which mottle the surface brightness distribution of both the lobes and the disk. For the present study we ignore these aspects of the homunculus and concentrate instead on the gross morphology and kinematics of the nebula, areas which an exploratory model can most clearly address.

Kinematical studies of the homunculus (Meaburn, Wolstencroft, & Walsh 1987, 1993) found strong evidence for collimated flow in the form of bipolar lobes and established an outflow velocity v for these lobes of $\sim$700 km s^{-1}. Assuming the distance of 2.5 kpc to η Car, the dynamical age of the system is $\sim$145 yr, a value which gives strong support for the hypothesis that nebula was produced by the eruption observed to begin in the 1840s. These same studies suggest that the nebula is inclined between 33° and 48° to the line of sight.

3. RELEVANT PHYSICS

Our models use the generalized interacting stellar winds scenario (Balick 1987; Icke 1988; Frank & Mellema 1994) in which nebular morphologies are explained by invoking the collision of stellar winds emanating from a central star, or "nucleus." The interaction of the winds produces two shocks, one moving outward into the circumstellar material and the other facing inward into the diluted stellar wind. In one-dimensional models, the outward-facing shock sweeps up a dense shell of circumstellar material whose properties fit observations of spherical planetary nebulae (PNs) quite well

[1] Department of Astronomy, University of Minnesota, Minneapolis, MN 55455; afrank@s1.msi.umn.edu, kd@ea.spa.umn.edu.
[2] Department of Astronomy, University of Washington, Seattle, WA 98195; balick@astro.washington.edu.

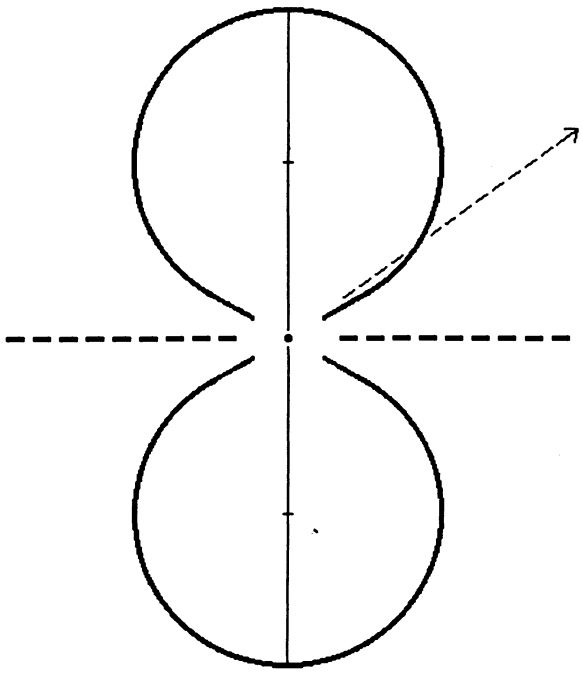

FIG. 1.—Shape of the homunculus. This is a sketch of a meridional plane cross section, in which the relative dimensions of the bipolar structure are consistent with various observations. A line pointing toward the upper right shows the approximate direction from which we see η Car. The latitude angle of this line of sight is consistent with the projected shape of the equatorial debris disk and with observed radial velocities of matter in the two lobes. The shape of each lobe and the relative size of the equatorial debris disk (a vertical dashed line in the sketch) are determined from the appearance of several images made with the *HST*.

(Volk & Kwok 1985; Marten & Schönberner 1991; Frank, Balick, & Riley 1990; Frank 1994; Mellema 1994). Just inside the outer shock is a contact discontinuity which is continuous in pressure but discontinuous in temperature and density. Inside the discontinuity is a hot bubble, mechanically heated by the stellar wind at the inner shock to a temperature $T_{\rm bub} = \frac{3}{32} m_{\rm H} v_w^2/k$ (Dyson & Williams 1980), where v_w is the speed of the stellar wind. (For the parameters appropriate to η Car, $T_{\rm bub} \approx 5 \times 10^6$ K in one-dimensional models.)

The interacting-winds scenario for spherical PNs can be generalized to model many types of aspherical nebulae by assuming that the circumstellar envelope is initially disklike, i.e., an equatorial enhancement of density exists as an initial condition (Balick 1987). Analytical studies (Kahn & West 1985; Icke 1988; Henney & Dyson 1992) and numerical simulations (Soker & Livio 1989; Mellema, Eulerink, & Icke 1992; Icke, Balick, & Frank 1992) show that gradients in the local acceleration (or ram pressure) can result in highly bipolar shock configurations. Recent radiation-gasdynamic models (Frank et al. 1993; Frank & Mellema 1994; Mellema & Frank 1994) have demonstrated that generalized interacting stellar wind models match observations of aspherical planetary nebula—including highly bipolar nebula—extremely well. The generalized interacting stellar wind model has also been applied to SN 1987A (Blondin & Lundqvist 1993). (Note that ring- or disklike mass distributions are astrophysically common; they are observed in young protoplanetary nebulae, at least one nova [Nova Cygni 1992], and, of course, many young stellar objects. A discussion of their origins lies beyond the scope of this paper.)

We shall assume that the observed disk formed around η Car prior to its outburst. In this *Letter* we explore the consequences of an "eruption wind" interacting with a previously formed toroidal environment assuming an isothermal evolutionary model.

4. COMPUTATIONAL METHODS AND RESULTS

The hydrodynamics of the wind-disk interaction was simulated using the two-dimensional local curvature diminishing (LCD) numerical gasdynamics code of Icke (1992). The LCD method is an explicit second-order–accurate Eulerian gasdynamics integrator developed especially for studying the evolution of concentric interacting axisymmetric stellar winds. This numerical code was used in previous studies of aspherical PN evolution (Icke, Balick, & Frank 1992; Frank 1992).

We have set the adiabatic index in our models to 1.01, which makes all shocks isothermal and reproduces the effect of strong cooling. This assumption is justified, since the cooling time for the shocks, t_c, will be short because of the high densities in the winds. The time t_c can be approximated as $(Cv_s)/(\rho_{\rm pre})$ (Kahn 1976), where v_s is the shock speed, $\rho_{\rm pre}$ is the preshock wind density, and $C = 6.0 \times 10^{-35}$ g cm^{-6} s^{-1}. For conditions appropriate to η Car the cooling time is always less than 3 yr, far less than the dynamical timescale of the nebula, $\sim$150 yr. We note that our simulations do not have the resolution to model accurately the width of the shell, which should be quite narrow because of the implied strong cooling.

The wind-wind interactions in our model are essentially momentum conserving (Dyson & Williams 1980), and isothermal models are, therefore, appropriate. In future investigations we will relax this assumption by including time-dependent forbidden-line cooling.

We assume that prior to the 1837 eruption, the wind emanating from the stellar surface is steady and characterized by

$$\rho(r, \theta) = \rho_0 \left(\frac{r_0}{r}\right)^2 \frac{1}{F(\theta)}, \tag{1}$$

$$V_r(r, \theta) = V_{r0} F(\theta), \tag{2}$$

where

$$F(\theta) = 1 - \alpha \left[\frac{1 - \exp(-2\beta \sin^2 \theta)}{1 - \exp(-2\beta)}\right]. \tag{3}$$

In equation (3) the parameter α controls the pole-to-equator density contrast in the wind, while β controls the shape of the wind. Low values of β produce distributions confined closer to the equator (although the minimum FWHM of the distribution is 90°). Large values of β produce spherical distributions with cones cut out from the polar regions. The choice of the form of equation (2) is somewhat arbitrary, where for simplicity we model the velocity contrast in the preeruption wind in such a way that the mass-loss rate in the wind is constant as a function of polar angle. Models of aspherical winds show that the mass-loss rate can at large distances be angle-dependent (Lamers & Pauldrach 1991; Bjorkman & Cassinelli 1992; Owocki, Cranmer, & Blondin 1994). We will explore these models as initial conditions in future investigations.

Although we have carried out more than 30 simulations, we will focus on only one which most closely matches the observations. We will call this run A; its initial conditions are $\dot{M} = 10^{-3}\ M_\odot$ yr^{-1}; $V_{r0} = 250$ km s^{-1}; $\alpha = 0.995$; $\beta = 2.3$ (FWHM = 120°); and $r_0 = 1 \times 10^{16}$ cm. In run A we allow

this "first" wind to fill the computational grid of 200 × 200 cells. (The radial length of a cell is 2.3×10^{15} cm.) Then, for 20 yr the mass-loss rate $\dot{M}$ is increased to 0.1 $M_\odot$ yr^{-1}, and the velocity is increased to $V_r = 750$ km s^{-1}. We assume and the eruption, or "second wind," is spherically symmetric (the effect of relaxing this assumption is discussed later). Subsequently the outflow from the star resumes its preeruptive mass-loss rate, which we consider a "third wind."

In run A the preeruptive wind is characterized by a pole-to-equator density contrast of 200 and a velocity contrast of 0.005. The low value of β used in model A produces a toroidal initial density distribution (as is observed in η Car).

For at least the first 150 years the momentum flux (pressure) is dominated by the impulse of the eruption. The posteruptive wind therefore has no significant effect on the development of the homunculus. So for simplicity in the computations we can assume that the third wind is spherically symmetric.

The posteruption evolution of the model homunculus is quite sensitive to the assumed preeruption flows, i.e., the initial conditions. Consequently we have explored initial conditions that bracket the most reasonable assumed conditions (as suggested by present observations). This permits us to investigate the extent to which the model results depend on assumptions at or before the time of the outburst.

Our simulations show that the progress of the forward-facing shock is strongly suppressed in the equatorial plane. However, in other directions the outer shock expands with higher velocities, and a thin, dense shell with a prolate, bipolar geometry forms quickly. The width and density of the shell are controlled by our assumption of strong postshock cooling. The detailed geometry of the bipolar shell would change if the computations were not isothermal; however, this affects mostly the shell thickness and not its overall dimensions or shape.

In Figure 2 (Plate L11) we present a gray-scale image of the log of the density in run A after 150 years. The ratio of the maximum width of the lobes to their maximum length, which is a rough measure of the morphology, is within 3% of that determined for the actual nebula based on geometrical deprojection (Fig. 1). In addition, the velocity in the lobes shows a "Hubble law" expansion pattern in which the shell velocity is essentially proportional to the distance from the central star—a pattern expected in momentum-conserving wind-blown bubbles (Shu et al. 1991). This pattern can be seen more clearly in Figure 3 (Plate L12), where we present four frames in the evolution of the model. In the current epoch the model shows that the lobes have a maximum expansion velocity of $V \sim 700$ km s^{-1}, which is well matched with the observations of Meaburn et al. (1987). The nebular evolution at the poles is essentially ballistic because the mass of the displaced preeruption wind is less than that ejected in the outburst (Koo & McKee 1992).

Projected onto the sky, the model homunculus has a size of 0.24 pc. From the measured angular size of *HST* images of 17″ this yields a predicted distance to η Car of 2.4 kpc, which compares well to the canonical value of 2.5 kpc.

Also, at the poles the calculations predict a characteristic density between the outer shock and the contact discontinuity (in which emission lines might be expected to arise) of less than 1×10^5 cm^{-3}, which might be verifiable through observations of forbidden-line ratios such as those of [S II]. This density is an upper limit (albeit a reasonable one), since the present computations assume that the shocks are isothermal and, therefore, that there is no upper limit on the density in the shock-compressed gas. Certainly the existence of [N II] emission observed in the homunculus argues that the density in the emitting region (which presumably arises in the recombination zone behind the shock) does not vastly exceed the critical density of about 10^5 cm^{-3}. Note that forbidden lines whose critical densities are of this order could be brightest along the leading edge of the lobes where the postshock density is *lowest*.

The shape (β) and density contrast (α) of the preeruptive wind as well as the maximum value of the wind velocity and density in the preeruption wind were varied in the other 30 simulations. We find that the model morphology, in particular the development of the tightly pinched wasp waist observed in the homunculus of η Car, is a sensitive function of the initial wind parameters α and β. The range $1 < \beta < 2.5$ produces model morphologies that best match the observations. For pole-to-equator density contrasts less than 100 no reasonable matches to the observations were achieved. We also find that dimensions of the model match those observed for the homunculus for maximum preeruption wind speeds less than 500 km s^{-1}.

The comparison between our model and one-dimensional estimates for plate-parallel isothermal shocks (see Blondin & Lundqvist 1993, eq. [2]) is intriguing. While the velocity of the shock is reasonably well matched at the pole, the velocity at the equator is off by more than a factor of 8. We have found a similar result using another numerical code. The difference between analytical and numerical shock velocities at the equator may be an artifact of resolution or boundary conditions. The analytical estimate for the equatorial shock velocity would carry the shell across only a few grid points in our simulation. However, the higher velocity seen in our simulations may have some validity in that the two shocks which bound the shell have opposite obliquities with respect to their preshock flows. This will cause a strong shear layer to form in the shell which may alter the momentum balance from that for a simple plane-parallel flow. We will explore this point again in the more detailed modeling we will undertake as the next step in this project.

5. DISCUSSION AND CONCLUSIONS

The most reasonable assumptions of initial conditions (based on archival observations) allows us to construct a hydrodynamic model for the evolution of η Car which satisfyingly conforms to the observations of its morphology and kinematics. We feel that we can safely conclude that a disk or gaseous toroid, formed before the outburst. Also, the density of the toroid must have been initially much more than one order of magnitude higher than its surroundings.

Future investigations will need to explore the parameter space of initial conditions more fully to determine the uniqueness of the match between theory and observations. The solution presented here is clearly not unique. Other sets of interacting stellar winds initial conditions are possible which could reproduce the morphology of η Car. In particular, models with variable mass-loss rate may also be able to provide appropriate confinement along the equator to reproduce the tight waist of the homunculus (although examination of Blondin & Lundqvist's eq. [2] shows that these models would still need density contrasts of order 10^2). The eventual use of gasdynamic models with realistic radiative energy losses (like those used in Frank et al. 1993; Frank & Mellema 1994; and Mellema & Frank 1994) will allow for the relaxation of the assumption of perfectly efficient cooling and, more important, will mean that "synthetic observations" of the spectra and

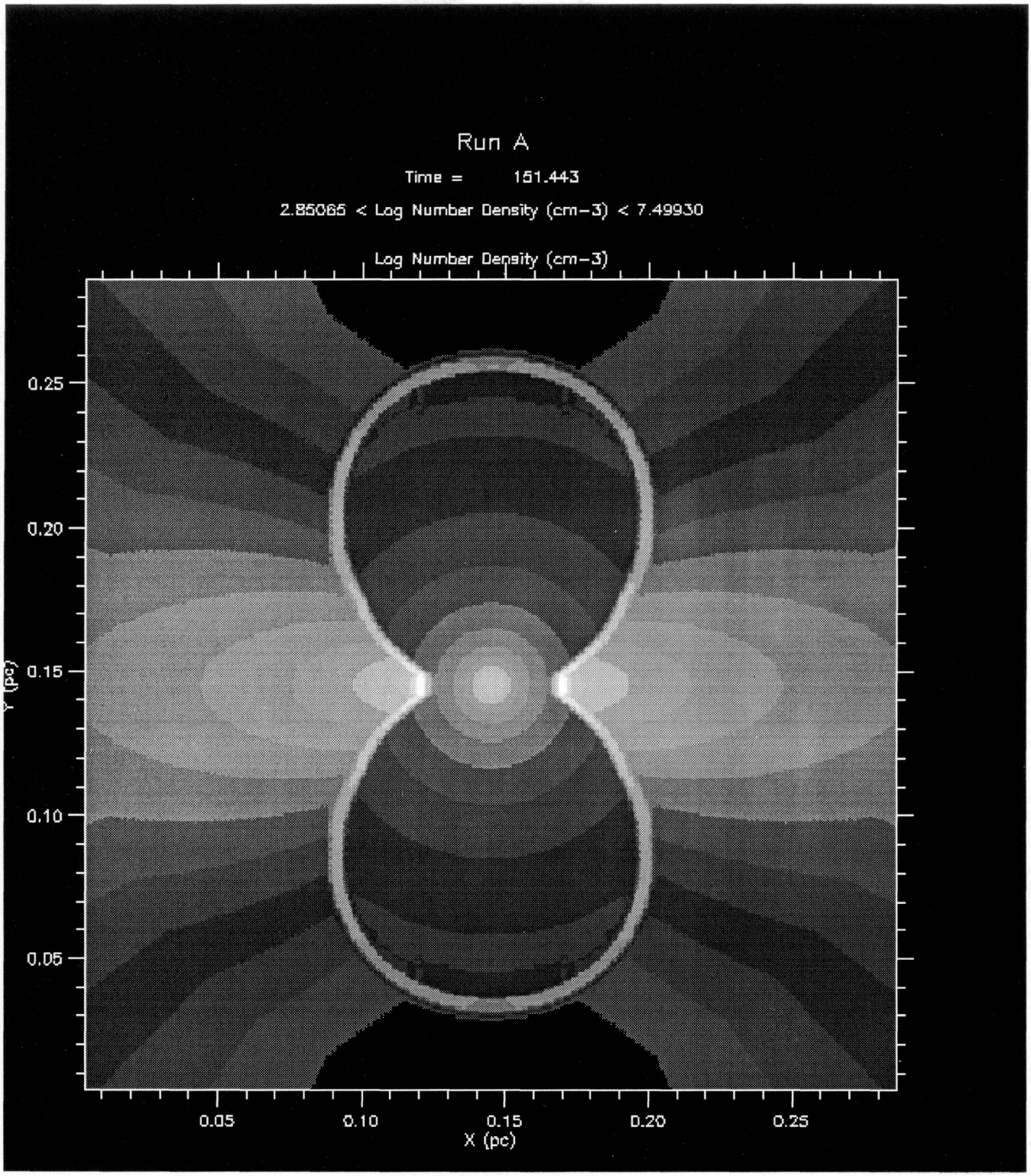

FIG. 2.—Gray-scale map of $\log_{10}$ number density in the run A simulation after 150 yr of evolution. The densities in the shell range from 10^7 cm^{-3} near the equator to 10^5 cm^{-3} near the poles. Note the morphological similarity between this image and Fig. 1.

FRANK, BALICK, & DAVIDSON (see 441, L79)

PLATE 12

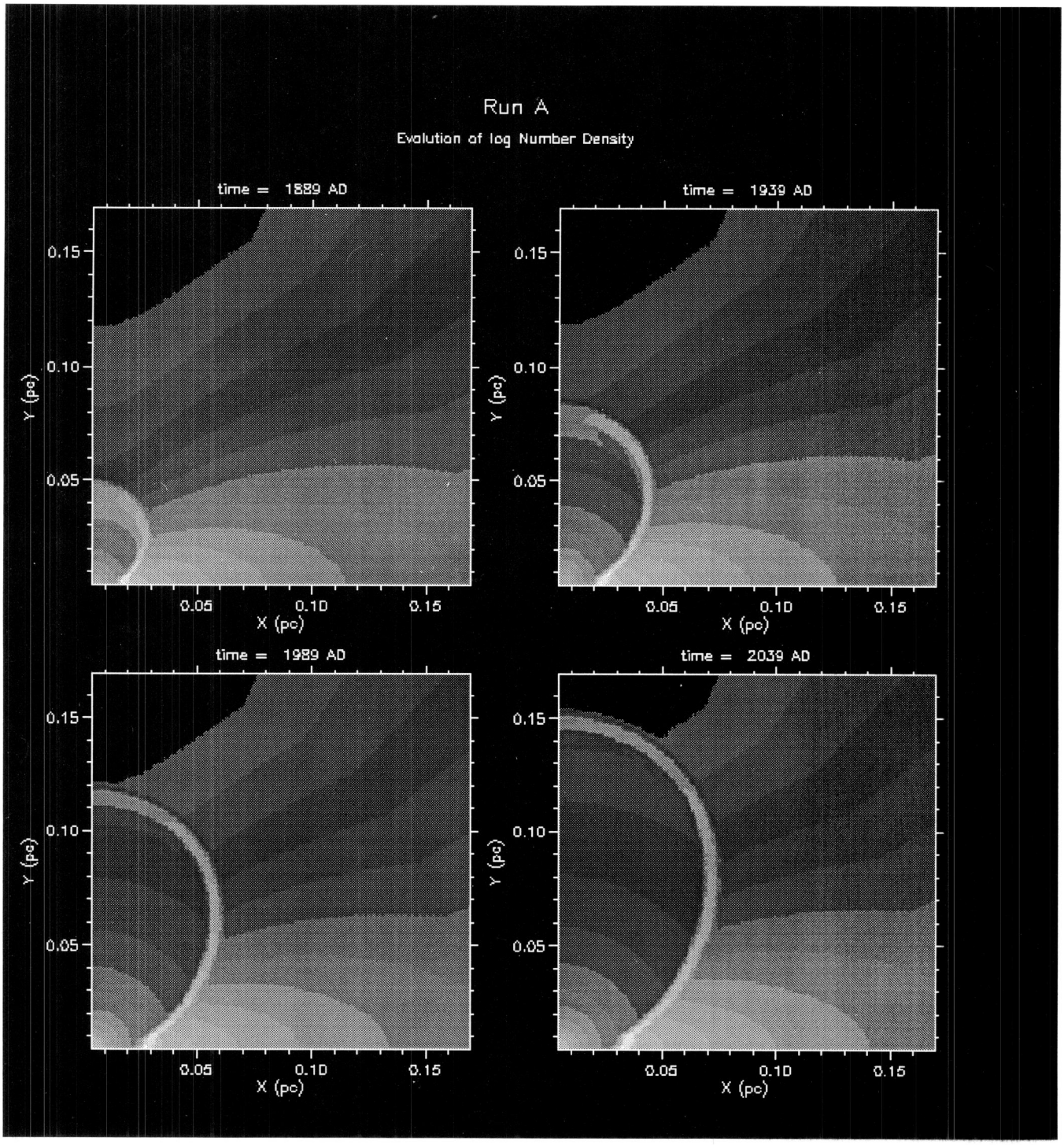

FIG. 3.—Gray-scale map of $\log_{10}$ number density in run A at four times in the evolution of the model spaced every 50 yr

kinematics as might be observed in a variety of spectral lines can be produced for detailed comparison with the actual homunculus.

We have not addressed the conspicuous microstructure of the homunculus of η Car in this *Letter*. It is natural to assume that the streaks, blobs, wormlike knots, and cometary tails which mottle the surface of the homunculus are the result of either dynamical or thermal instabilities. We note that shear layers along the inner surface of the dense shell occur naturally in our models and may produce Kelvin-Helmholtz instabilities. The posteruption wind may play a role in the development of these and perhaps other (Rayleigh-Taylor or Vishniac blast wave; Ryu & Vishniac 1991) instabilities. If the posteruption wind has a high enough velocity, then some acceleration (perhaps driven by thermal pressure from an incomplete shock) may occur which could drive these instabilities with growth rates comparable to the evolutionary timescale of the homunculus. The investigation of these effects will be taken up in subsequent studies.

Finally, we note the intriguing possibility that the homunculus may consist not of bipolar lobes but instead of expanding spherical caps, as has been suggested by Currie et al. (1994). A similar model was used in the study of molecular outflows of YSOs by Shu et al. (1991). Such a scenario would be a further generalization of the interacting stellar winds paradigm and could be easily simulated with the numerical code used in this investigation.

We wish to thank the refereee Jon Bjorkman for his many insightful comments on the text. We wish to thank Mordecai-Mark Mac Low for fruitful discussions concerning η Car and the Vishniac instability. A. F wishes to thank Garrelt Mellema for his guidance in the development of the visualization software used in this paper. This work was supported by NASA through grant NAGW-2548, by the NSF through grant AST-9100486, and by the University of Minnesota Supercomputer Institute.

REFERENCES

Balick, B. 1987, AJ, 94, 671
Bjorkman, J. E., & Cassinelli, J. P. 1992, ApJ, 409, 429
Blondin, J. M., & Lundqvist, P. 1993, ApJ, 405, 337
Currie, D. G., Dowling, D. J., Avizonis, P. V., Hester, J. J., Scowen, P. A., Groth, E. J., & Idt, W. 1994, BAAS, 26, 914
Damineli Neto, A., Viotti, R., Baratta, G. B., & de Araujo, F. X. 1993, A&A, 268, 183
Davidson, K. 1993, in ASP Conf. Ser. 35, Massive Stars: Their Lives in the Interstellar Medium, ed. J. Cassinelli & E. B. Churchwell (San Francisco: ASP), 483
Dyson, J. E., & Williams, D. 1980, The Physics of the Interstellar Medium (New York: Wiley)
Ebbets, D., Garner, H., White, R., Davidson, K., Malumuth, E., & Walborn, N. 1994a, in Proc. 34th Herstmonceaux Conf., Circumstellar Media in the Late Stages of Stellar Evolution (Cambridge: Cambridge Univ. Press), in press
———. 1994b, in preparation
Frank, A. 1992, Ph.D. thesis, Univ. Washington
———. 1994, AJ, 107, 534
Frank, A., Balick, B., Mellema, G., & Icke, V. 1993, ApJ, 404, L25
Frank, A., Balick, B., & Riley, J. 1990, AJ, 100, 1903
Frank, A., & Mellema, G. 1994, ApJ, 430, 800
Henney, W. J.., & Dyson, J. E. 1992, A&A, 261, 301
Hester, J. J., Light, R. M., Westphal, J. A., Currie, D. G., Groth, E. J., Holtzman, J. A., Lauer, T. R., & O'Neil, E. J. 1991, AJ, 102, 654
Humphreys, R. M., & Davidson, K. 1994, PASP, 106, 1025
Icke, V. 1988, A&A, 202, 177
———. 1992, A&A, 251, 369
Icke, V., Balick, B., & Frank, A. 1992, A&A, 253, 224
Kahn, F. D. 1976, A&A, 50, 145
Kahn, F., & West, K. A. 1985, MNRAS, 212, 837
Koo, B., & McKee, C. F. 1992, ApJ, 388, 93
Lamers, H. J. G. L. M. 1989, in The Physics of Luminous Blue Variables, ed. K. Davidson, A. F. J. Moffat, & H. J. G. L. M. Lamers (Dordrecht: Kluwer), 135
Lamers, H. J. G. L. M., & Pauldrach, A. W. A. 1991, A&A, 244, L5
Maeder, A. 1989, in The Physics of Luminous Blue Variables, ed. K. Davidson, A. F. J. Moffat, & H. J. G. L. M. Lamers (Dordrecht: Kluwer), 15
Marten, H., & Schönberner, D. 1991, A&A, 248, 590
Meaburn, J., Walsh, J. R., & Wolstencroft, R. D. 1993, A&A, 268, 163
Meaburn, J., Wolstencroft, R. D., & Walsh, J. R. 1987, A&A, 181, 333
Mellema, G. 1994, A&A, in press
Mellema, G., Eulerink, F., & Icke, I. 1992, A&A, 252, 718
Mellema, G., & Frank, A. 1994, A&A, in press
Owocki, S. P., Cranmer, S. R., & Blondin, J. M. 1994, ApJ, 424, 887
Pauldrach, A. W. A., & Puls, J. 1990, A&A, 237, 409
Ryu, D., & Vishniac, E. T. 1991, ApJ, 368, 411
Shu, F., Ruden, S. P., Lada, C., & Lizano, S. 1991, ApJ, 370, L3
Soker, N., & Livio, M. 1989, AJ, 339, 268
Volk, K., & Kwok, S. 1985, A&A, 153, 79